

On the Vulnerability of Concept Erasure in Diffusion Models

Lucas Beerens^{*1}, Alex D. Richardson^{*1,2}, Kaicheng Zhang^{*1}, Dongdong Chen³
^{*} Equal contribution

¹ School of Mathematics and Maxwell Institute, University of Edinburgh, Edinburgh, UK

² School of Physics and Astronomy, University of Edinburgh, Edinburgh, UK

³ School of Mathematical and Computer Sciences, Heriot-Watt University, Edinburgh, UK

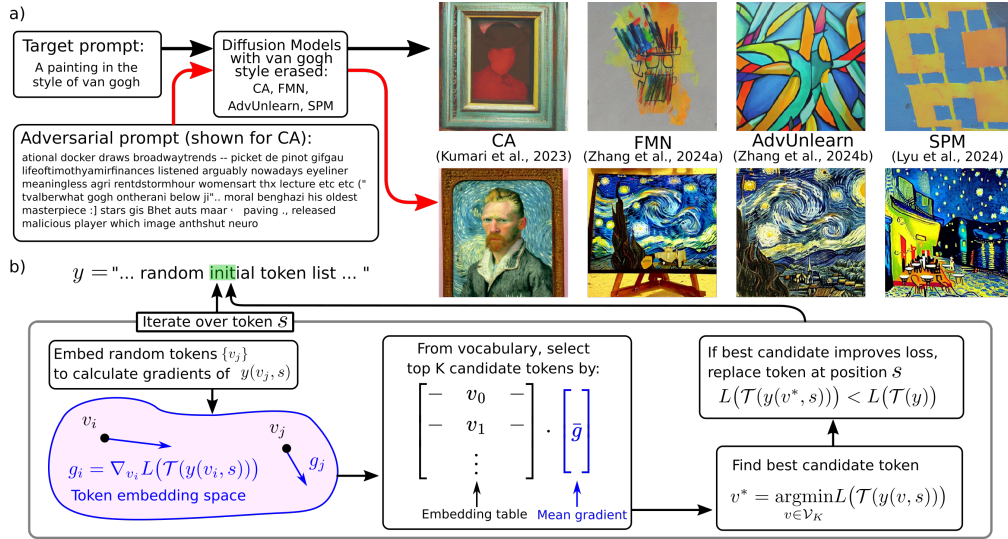


Figure 1: **a)** Examples of restored concepts from models unlearned on van Gogh painting style. **b)** The update schematic of RECORD, which uses a linear gradient approximation to obtain a small set of candidate tokens, and then updates the prompt with respect to their exact gradients.

Abstract

The proliferation of text-to-image diffusion models has raised significant privacy and security concerns, particularly regarding the generation of copyrighted or harmful images. In response, several concept erasure (defense) methods have been developed to prevent the generation of unwanted content through post-hoc finetuning. On the other hand, concept restoration (attack) methods seek to recover supposedly erased concepts via adversarially crafted prompts. However, all existing restoration methods only succeed in the highly restrictive scenario of finding adversarial prompts tailed to some fixed seed. To address this, we introduce **RECORD**, a novel coordinate-descent-based restoration algorithm that finds adversarial prompts to recover erased concepts *independently* of the seed. Our extensive experiments demonstrate RECORD consistently outperforms the current restoration methods by up to 17.8 times in this setting. Our findings further reveal the susceptibility of unlearned models to restoration attacks, providing crucial insights into the behavior of unlearned models under the influence of adversarial prompts. The code for

RECORD is available at [available upon publication].
Note: this paper may contain offensive or upsetting images

1 Introduction

Text-to-Image Diffusion models have recently garnered significant attention for their ability to generate high-quality images from natural language inputs [30, 36]. However, because these models are trained on vast and diverse datasets that may contain harmful or undesirable content, their proliferation raises substantial ethical and safety concerns, particularly over the generation of private, copyrighted and harmful content [3, 35]. Pre-filtering undesired images from the training dataset is often considered impractical due to the sheer size of these datasets, as well as the necessity to re-train the model from scratch. Consequently, much research has pursued post-hoc approaches aiming to remove the influence of undesired content from trained models via low-cost finetuning, while preserving the generation quality of other non-erased concepts [8, 10–12, 18, 20, 25, 42, 43, 45, 46]. This is commonly referred to as *concept erasure*, a subfield of *machine unlearning* [19].

However, it is well-known that neural networks are susceptible to adversarial attacks: small perturbations to an input can induce a well-trained model to produce any pre-determined outputs without altering the model itself [1, 5, 21]. This vulnerability raises similar concerns in the context of concept erasure. Indeed, recent studies have largely demonstrated the feasibility of eliciting unlearned models to re-generated the erased concepts via white-box optimization-based attacks [3, 47]. Although the reliance on a white-box scenario limits the practicality of these attacks by external adversaries on closed-sourced models, these methods are instrumental in auditing the robustness in concept erasure research. We refer to this class of attack methods as *concept restoration*.

The existing concept restoration methods rely on projecting the discrete text prompts into a continuous and differentiable space to enable gradient-based optimization [3, 47]. However, projection-based adversarial attacks have been shown to perform poorly on large language models (LLMs) [2]. Consequently, all existing restoration methods can only identify adversarial prompts tailored to a specific seed, which an outside adversary likely has no control over. In particular, our experiments demonstrate that these methods almost completely fail when evaluating their optimized prompts with different random seeds. In this paper, we propose **RECORD (Restoring Erased Concepts via Coordinate Descent)**, a white-box coordinate-descent algorithm that employs a two-stage optimization scheme that negates the need for projection. To the best of our knowledge, RECORD is the first concept restoration method to consistently find non-seed-specific adversarial prompts that can restore a whole *distribution* of images of an erased concept, achieving a 17.8-fold improvement over the existing state-of-the-art restoration methods. Examples of restored images are represented in Table 1

Our investigations also reveal crucial insights into the fundamental vulnerability of the unlearned models. Notably, for *any* arbitrary initialization in the prompt embedding space, our findings suggest there always exist nearby embeddings that can trigger the generation of erased concepts, suggesting possible adversarial prompts exist almost everywhere in the prompt embedding space. Furthermore, embeddings initialized close to the embeddings of exact descriptions of the erased concept tend to move away from those embeddings during optimization. This suggests most existing unlearning methods only suppress the generation of the erased concept when using its exact description or its semantically similar versions.

2 Background

2.1 Text-to-Image Diffusion Models

Diffusion Models are a class of generative model that generate images from text by learning to reverse the forward diffusion process. Starting with Gaussian noise $x_T \sim \mathcal{N}(0, \mathbf{1})$, a trained denoiser, commonly a U-Net [31] or Vision Transformer [6], iteratively denoises x_T over the interval $t \in [0, T]$ until a clear image x_0 is reached. By conditioning on prompt embeddings $c = \mathcal{T}(y)$, where y is some natural language prompt, text-to-image generation is achieved. \mathcal{T} is a pre-trained text encoder, commonly CLIP [28] or BLIP [24]. In practice, many popular diffusion models, such as Stable Diffusion [30], perform the denoising in a latent space $z_t = \mathcal{E}(x_t)$. The denoiser ϵ_θ parameterized by

Restoration Method	Erasure Method					
	ESD [10]	FMN [45]	AC [20]	SPM [25]	UCE [11]	AdvUnlearn [46]
P4D [3]						
UD [47]						
RECORD						

Table 1: Generated images of erased concepts (van Gogh paintings) using prompt attacks. Each image column of the same concept is generated using the same latent initialization.

θ can then be trained by optimizing

$$\operatorname{argmin}_{\theta} \mathbb{E}_{z \sim \mathcal{E}(x), t, \epsilon \sim \mathcal{N}(0,1), c} \|\epsilon - \epsilon_{\theta}(z_t, t, c)\|_2^2.$$

where z_t is obtained by applying the forward diffusion process to the clean latent z_0 using the Gaussian noise ϵ .

2.2 Prompt Tuning

Manipulating prompts to elicit specific behaviors from language models, also known as prompt tuning, is an important topic in Natural Language Processing research. [7] introduced HotFlip, generating adversarial examples through minimal character-level flips guided by gradients. Extending this, [39] developed Universal Adversarial Triggers—input-agnostic token sequences optimized by using first order Taylor-expansion around the current token to select candidate tokens for exact evaluation. [34] presented AutoPrompt, designed to automatically generate prompts for various use cases. Addressing the lack of fluency in these prompts, [33] introduced FluentPrompt, incorporating fluency constraints and using Langevin Dynamics combined with Projected Stochastic Gradient Descent, where projection is done onto the set of token embeddings. [41] developed PEZ, an algorithm inspired by FluentPrompt, allowing for prompt creation in both text-to-text and text-to-image applications. In text-to-image models, [9] applied Textual Inversion, learning “pseudo-words” in the embedding space to capture specific visual concepts. Further advancements include GBDA [13], enabling gradient-based optimization over token distributions using the Gumbel-Softmax reparametrization [16] to stay on the probability simplex, and ARCA [17], optimizing discrete prompts via an improvement to AutoPrompt. ARCA will inspire our method.

2.3 Concept Restoration

Recent methods designed to restore erased concepts from unlearned models often leverage advanced optimization techniques similar to prompt tuning. Concept Inversion (CI) [27] introduces a new token with a learnable embedding to represent the erased concept, which is learned to minimize the reconstruction loss during denoising. This is a direct application of Textual Inversion [9] from prompt tuning to the concept restoration paradigm. Prompting Unlearned Diffusion Models (PUND) [14] enhances this approach by iteratively erasing and searching for the concept by also updating model parameters, improving transferability across models.

Other methods focus on discrete token optimization. UnlearnDiffAtk (UD) [47] performs optimization over token distributions, similar to GBDA [13], but utilizes projection onto the probability simplex instead of the Gumbel-Softmax reparameterization. Prompting4Debugging (P4D) [3] optimizes

prompts in the embedding space and projects onto discrete embeddings, akin to the approach used in PEZ [41]. Additionally, Ring-A-Bell [38] constructs an empirical representation of the erased concept by averaging embedding differences from prompts with and without the concept, then employs a genetic algorithm to optimize the prompt.

3 Method

3.1 Motivation: Vulnerability of Machine Unlearning

Vulnerability Verifying whether a model has truly unlearned a concept is challenging. To assess the effectiveness of the unlearning process, we consider an unlearned denoiser $\epsilon_{\theta'}$ to be robust if it consistently fails to generate the erased content and produce images significantly different from those generated by the original model ϵ_{θ} when subjected to any adversarial prompt and any latent initialization. Therefore, this work focuses on measuring the degree to which the unlearned model has diverged from the original model concerning the erased content. To achieve this, we propose a loss function similar to [3]

$$L(c) = \mathbb{E}_{t,z} \left[\left\| \epsilon_{\theta'}(z_t, t, c) - \epsilon_{\theta}(z_t, t, c_{\text{target}}) \right\|_2^2 \right], \quad (1)$$

where $c = \mathcal{T}(y)$, $c_{\text{target}} = \mathcal{T}(y_{\text{target}})$, z_t is obtained through the forward diffusion process with z_0 sampled from the target data distribution p_{target} . y_{target} is the target prompt. The subsequent concept restoration attacks can be performed by minimizing this loss and finding the adversarial text prompt

$$y^* = \underset{y}{\operatorname{argmin}} L(\mathcal{T}(y)).$$

This formulation is similarly applicable to erasure methods which unlearns the text encoder \mathcal{T} .

Some literature recommends the use of a Gaussian noise ϵ in place of the original model $\epsilon_{\theta'}$, citing the reduced computational costs [47]. Empirically we observe the loss function from equation (1) improves the effectiveness of concept restoration attacks, as the predictions of the original model ϵ_{θ} act as a more informative surrogate than the Gaussian noise. We refer the readers to appendix A for more detailed discussions and experimental results.

This paper considers two types of restoration attacks to assess the vulnerability of unlearned models:

- **Prompt embedding attacks:** In this setting, concept restoration is achieved by directly perturbing the prompt embedding c to minimize the loss function defined in equation (1). With the prompt embedding space being continuous and differentiable, finding non-seed-specific adversarial prompts poses an easier task. However, precise inversions from embeddings back to prompts are not guaranteed to exist, and embedding attacks are less practicable in most scenarios. Here we use these attacks as ablation studies in section 4.3 for analyzing concept erasure vulnerability under small continuous perturbations, and in appendix A for examining different loss functions.
- **Prompt attacks:** Directly perturbing prompt tokens to restore concepts is significantly more challenging due to their discrete and non-differentiable nature. Consequently, existing restoration methods primarily focus on seed-specific adversarial prompts and struggle to find general adversarial prompts effective across all seeds. To overcome this limitation, we introduce **RECORD** (Restoring Erased Concepts via Coordinate Descent) for carrying out robust non-seed-specific concept restoration attacks.

3.2 RECORD

The coordinate-descent-based two-stage approach employed by RECORD iteratively optimizes the prompt one token at a time while fixing all other tokens in the prompt sequence. The algorithm first initializes a random token sequence $y = [y_1, \dots, y_S]$ of length S , and iteratively perform N passes over y . In each pass, a random permutation of the token positions is generated to mitigate positional bias during updates. For each position s in the permuted sequence, the algorithm samples a batch of K images $z_0^{[n]}$ and corresponding timesteps $t^{[n,s]}$. Candidate tokens v for position s are then selected by sampling J random tokens. Since computing the exact expectation over all latents and timesteps is intractable, we approximate the $L(y)$ from equation (1) as:

$$\hat{L}(y, \mathcal{Z}) = \sum_{(z_t, t) \in \mathcal{Z}} \left\| \epsilon_{\theta'}(z_t, t, \mathcal{T}(y)) - \epsilon_{\theta}(z_t, t, \mathcal{T}(y_{\text{target}})) \right\|_2^2, \quad (2)$$

Algorithm 1 Pseudocode of RECORD.

```
#  $\theta'$ : original model;  $\theta$ : unlearned model
#  $y_{\text{target}}$ : target prompt
#  $J$ : gradient samples;  $K$ : candidates
#  $S$ : sequence length;  $N$ : passes
#  $R$ : reference set;  $E$ : embedding table

Random token sequence  $y$  of length  $S$ : # initialization
for n=1 to N: # load N passes
  # Shuffle
  Random permutation  $\pi$  of positions  $\{1, \dots, S\}$ 

  for  $s$  in  $\pi$ :
    # sample data
    Sample batch  $\mathcal{Z}$  of noise images and timesteps
    # candidate selection
    Sample  $J$  random tokens  $\{v_j\}$ 
    Compute gradients  $\bar{g} = \frac{1}{J} \sum_{j=1}^J \nabla v_j \hat{L}(y(v_j, s), \mathcal{Z}(n, s))$ 
    Score all tokens: scores  $\leftarrow E \bar{g}$ 
    Select top  $K$  tokens  $\mathcal{V}$  based on scores

    # candidate evaluation
     $\hat{v}^* = \arg \min_{v \in \mathcal{V}} \hat{L}(y(v, s), \mathcal{Z})$  # best candidate
    # coordinate descent
    if  $\hat{L}(y(\hat{v}^*, s), \mathcal{R}) < \hat{L}(y, \mathcal{R})$ :
      Update  $y \leftarrow y(\hat{v}^*, s)$ 
Return: optimized prompt  $y$  for restoring erased concepts
```

where \mathcal{Z} is a sampled batch of noised images and their corresponding timesteps. The gradient g of \hat{L} with respect to the candidate token embeddings can thus be computed as:

$$g_j = \nabla_{c_j} \hat{L}(y(c_j, s), \mathcal{Z}(n, s)).$$

The average gradient $\bar{g} = \frac{1}{J} \sum_{j=1}^J g_j$ serves as a linear approximation to \hat{L} with respect to the entire prompt embedding space. By multiplying the embedding table E with \bar{g} , we efficiently score all possible tokens and select the top V candidates for exact evaluation. During the evaluation and subsequent update of y_s , we employ a greedy strategy: A candidate token \hat{c}^* is only accepted if it improves the loss, i.e. when $\hat{L}(y(\hat{c}^*, s), \mathcal{R}) < \hat{L}(y, \mathcal{R})$. This update process iterates for all positions in the permutation and repeats for N passes, progressively enhancing the token sequence over time. Since each accepted token replacement strictly decreases the loss and the number of possible token sequences is finite, the algorithm is guaranteed to converge to a coordinate-wise local minimum. A pseudocode can be found in Algorithm 1.

Although the RECORD algorithm as stated above is tailored for attacking denoiser-based erasure methods, it can be easily adapted to text-encoder-based erasure methods by replacing $\epsilon_{\theta'}(z_t, t, \mathcal{T}(y))$ with $\epsilon_{\theta}(z_t, t, \mathcal{T}'(y))$ in equation (2), where \mathcal{T}' is the unlearned text encoder.

4 Experiments

We extensively compare RECORD against the two current state-of-the-art methods in the literature, P4D [3] and UD [47], on text-to-image diffusion models unlearned with both denoiser-based (ESD [10], ED [43], SH [42], FMN [45], CA [20], SPM [25], SalUn [8], UCE [11], and RECE [12]) and text-encoder-based (AdvUnlearn [46]) concept erasure methods. Although there are other black-box methods that suppress generation of harmful content without post-hoc training the denoiser or the text encoder [15, 23, 32, 44], such methods target a fundamentally different adversary, e.g. one with only API access, and cannot exploit internal gradients or weights of the unlearned model. Including them here would not yield an apple-to-apple evaluation of concept erasure under full model access. Unless stated otherwise, all experiments reported in this section aim to find non-seed-specific adversarial prompts, instead of the seed-specific setting commonly investigated in prior literature. The weights of the unlearned models in this section are obtained from [12, 46], which uses Stable Diffusion 1.4 [30] as the base model. The erased concepts include art style (van Gogh), objects (church, garbage truck, parachute) and nudity.

4.1 Evaluation metrics

Most text-to-image diffusion models can generate a far broader range of objects and styles than any single image classifier is capable of classifying. Prior work therefore evaluates concept erasure and restoration methods by ensembling multiple classifiers, each with its own architecture, training data, and preprocessing method, introducing potential inconsistencies. To address this issue, as well as to improve reproducibility and ease replication, we adopt a single, unified zero-shot diffusion classifier (Stable Diffusion v2.1) [4, 22] to classify the generated images. The classification results are obtained by computing

$$y^* = \operatorname{argmin}_{y_i \in Y} \mathbb{E}_t \|\epsilon - \epsilon_\theta(z_t, t, \mathcal{T}(y_i))\|_2^2,$$

where the timestep t is uniformly sampled from $U(0, T)$, $Y = \{y_1, y_2, \dots, y_n\}$ is a set of n classification classes. The expectation is computed over 10 samples, which in our experience is sufficient to provide accurate classification results. For art style and object attacks, we build sets of 50 classes using prompt templates ‘a painting in the style of {artist_name}’ and ‘a photorealistic image of {object}’, where the artist names are randomly chosen from a list of famous painters, e.g. Leonardo Da Vinci, and object names are from the classification classes of YOLOv3 [29]. For nudity attacks, a set of 4 classes are built with the same template as the object attacks. For all attacks, we also additionally add one empty class, ‘’, which helps the classifier capture images that fall significantly outside the distributions of the specified classes. All results presented in this section are computed on 500 images generated by the corresponding erased models and restoration attacks. We report the Attack Success Rate (ASR) in percentage, calculated by dividing the number of images classified as the target (erased) class by the total number of generated images. We attach the classification accuracy of the zero-shot diffusion classifier on images generated by the baseline model in Table 2, which serves as references for the ASRs of the corresponding concepts.

Erased concept	Van Gogh	Church	Garbage Truck	Parachute	Nudity
Accuracy	99.4	98.8	93.4	84.0	87.6

Table 2: The accuracy of Stable Diffusion 2.1 in zero-shot classifying images generated by Stable Diffusion 1.4

4.2 Prompt Attacks

In this experiment, each restoration method (P4D[3], UD[47], RECORD) aims to find 64-token-long non-seed-specific adversarial prompts starting from a randomly initialized prompt sequence, except UD. Since UD optimizes on a token distribution, we follow their original initialization strategy by setting the first few tokens to be the target prompt, and initializing the rest of the tokens from a uniform distribution for all tokens. Without this type of initialization UD does not achieve any significant results. Each restoration methods is evaluated by first creating 50 adversarial prompts. Each prompt is then used to create 10 images, totaling 500 images per method to be used for ASR calculations. For RECORD, we use $N = 20$ passes through the token list, a batch size of 1 image each, and $J = 64$ samples for the candidate selection. The chosen candidate set has size $K = 64$. These numbers are chosen to make the best use the available VRAM of an 80GB H100 GPU. We include results on how runtime scales with number of tokens (Table 3). The runtime of RECORD is competitive despite its parameters are not tuned to minimize runtime. UD has a shorter runtime due to its use of loss (3). This loss can also be used by RECORD, which is a tradeoff between marginal attack performance gain and runtime, as investigated in Appendix A.

Number of tokens	Restoration Method Runtime/ <i>s</i>		
	P4D	UD	RECORD
8	2059 ± 49	305 ± 7	235 ± 16
16	2050 ± 34	429 ± 7	464 ± 18
32	2070 ± 22	638 ± 39	929 ± 16
64	2079 ± 22	1003 ± 50	1859 ± 15

Table 3: The runtime comparison is computed over 10 runs. Both K and J are set to the number of tokens.

Erased Concept	Restoration Method	Erasure Method						
		ESD [10]	FMN [45]	AC [20]	SPM [25]	UCE [11]	AdvUnlearn [46]	RECE [12]
van Gogh	No attack	3.4	17.6	32.2	45.4	52.8	0.8	13.4
	P4D [3]	6.6	27.2	49.8	54.8	67.2	2.8	50.8
	UD [47]	5.4	25.4	17.0	34.6	42.8	2.8	10.0
	RECORD	64.0	76.8	94.0	95.6	97.6	33.0	89.0
Erased Concept	Restoration Method	Erasure Method						
		ED [43]	ESD [10]	SalUn [8]	SH [42]	SPM [25]	AdvUnlearn [46]	RECE [12]
Church	No attack	2.0	20.2	4.4	1.0	84.6	1.6	6.8
	P4D [3]	16.0	24.6	28.8	3.4	51.6	7.0	8.2
	UD [47]	2.6	4.8	5.4	4.4	22.8	1.4	6.8
	RECORD	61.2	75.2	71.4	8.6	92.2	57.0	46.4
Garbage Truck	No attack	20.4	6.2	9.0	9.2	28.4	0.2	1.6
	P4D [3]	9.4	18.8	21.0	0.4	35.8	34.2	5.6
	UD [47]	16.0	3.8	17.0	4.4	29.2	0.2	1.2
	RECORD	40.8	38.8	58.0	1.0	66.4	50.0	17.0
Parachute	No attack	3.8	0.8	1.2	2.2	29.8	0.2	4.8
	P4D [3]	5.6	11.6	20.6	0.6	15.6	2.0	4.2
	UD [47]	3.0	2.4	2.4	1.0	6.8	1.2	3.2
	RECORD	15.4	44.6	48.8	2.0	60.4	35.6	10.0
Nudity	No attack	7.0	49.2	1.8	2.0	49.6	38.4	35.4
	P4D [3]	2.0	37.6	9.8	9.6	28.8	17.0	15.2
	UD [47]	4.0	19.2	4.2	2.0	2.5	14.2	19.4
	RECORD	2.4	70.6	9.0	21.2	69.0	39.2	38.8

Table 4: Attack success rate (%) for models with the concepts (van Gogh style, Church, Garbage Truck, Parachute, Nudity) erased, compared between the restoration methods P4D [3], UD [47], and RECORD (ours). The best and second-best values are marked in **red** and **blue**, respectively.

The results from Table 4 show that P4D and UD struggle to find non-seed-specific adversarial prompts, with some performing even worse than the no attack baseline, underscoring their ineffectiveness when the seed is not fixed during optimization. On the other hand, RECORD consistently outperforms P4D and UD by up to 17.8 times (see the AdvUnlearn-Parachute result), except for a few minor exceptions. In particular, AdvUnlearn is quite resilient against P4D and UD with single digit ASR on most concepts, while RECORD is able to achieve an ASR of at least 33% for all concepts. SH models are very robust against all concept restoration attacks, but this comes at a significant cost of

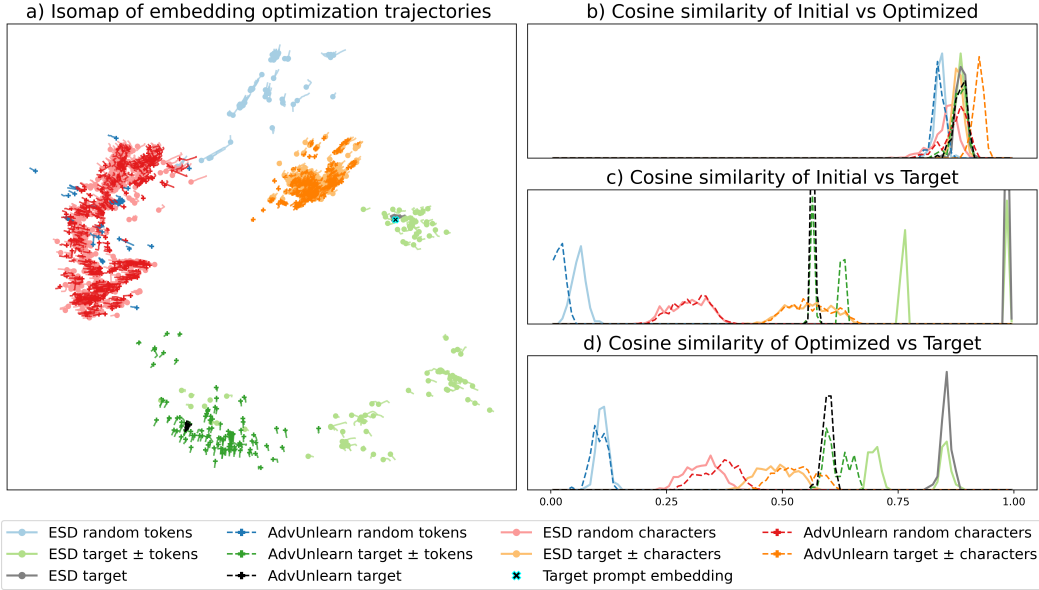


Figure 2: Behavior of the prompt embeddings during prompt embedding attacks. **a)** Isomap projection of the optimization trajectories of the prompt embeddings during embedding attacks. The rest of the figures are cosine similarity histograms between **b)** the initial and target embeddings; **c)** the optimized and target embeddings; **d)** the optimized and initial embeddings. Target prompt embedding is “a painting in the style of van Gogh” encoded by the non-unlearned text encoder from the baseline model. All data points shown here can successfully generate the erased concept from the unlearned models in the non-seed-specific setting.

the generation quality of other non-erased concepts, which has been investigated and discussed in detail by [46].

Example images on van Gogh style can be found in Table 1, as well as in Appendix B for other erased concepts. We also provide an ablation study on the number of tokens K in Appendix C, where we demonstrate RECORD maintains excellent performance even with only 16 tokens (Tables 11,12).

4.3 Prompt embedding manifolds

We carefully assess the vulnerability of the concept erasure methods against small perturbations by examining the optimization behaviors with different initializations for prompt *embedding* attacks. We present a 2D isomap [40] projection (Figure 2a) to visualize the optimization trajectories of prompt embeddings and histograms of the cosine similarity between initial, optimized, and target embeddings (Figure 2b-d). The use of cosine similarity is motivated by the observation that text embeddings typically lie on a hypersphere. We note that our observations are consistent across all denoiser-based concept erasure methods examined, but for clarity we only show ESD (denoiser based) and AdvUnlearn (text encoder based) for comparison. We consider four different initialization schemes: In the first two schemes, initial prompts are sampled “close” to the target prompt of the erased concept by padding the target prompt with random characters (\pm characters) or by padding and replacing random tokens (\pm tokens) of random lengths. On the other hand, initial prompts are sampled “far” from the target prompt by uniformly sampling random characters or tokens.

Embeddings initialized either close or far from the target prompt can successfully restore the erased concept with short optimization trajectories (Figure 2a and b). In particular, prompts initialized in the “far” region do not approach the cluster that contains the target embedding projection. This suggests that, in any region of the prompt embedding space, **there almost always exists a nearby prompt embedding capable of restoring the erased concept**. In other words, unlearned models are generally vulnerable to small perturbations to the embedding of any arbitrary prompt. Furthermore, the comparison between the initial and optimized text embeddings (Figure 2c and d) reveals that

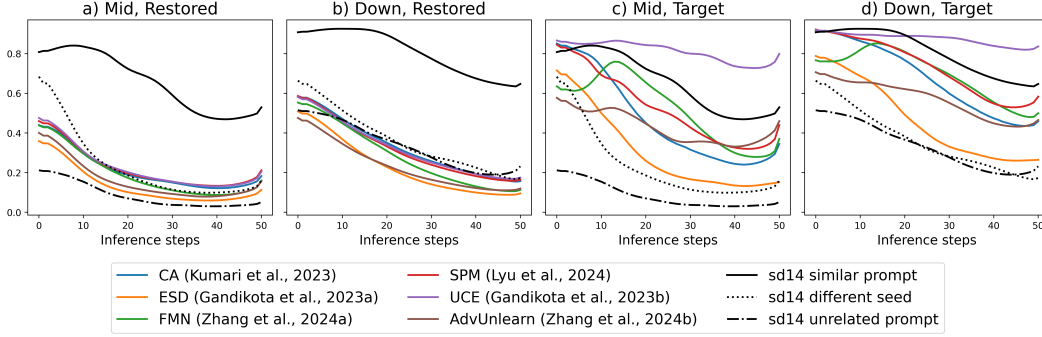


Figure 3: Cosine similarities of trajectories of U-Net bottleneck features between unlearned and baseline models during inference, using RECORD-restored (a-b) and non-perturbed (c-d) target prompts. These are compared with the black-colored baseline inference trajectories of semantically related prompts. We borrow the nomenclature from literature [37] and use "Mid" and "Down" to represent the bottleneck and final downsampling layers of the U-Net, respectively. In this particular case, we use a target prompt "a painting in the style of van Gogh", a similar prompt "a painting of starry night by van Gogh", and an unrelated prompt "a photorealistic image of a sports car" as reference trajectories of semantically similar and unrelated text prompts. All generations use the same seed and thus the same latent initialization, unless noted otherwise. For (a-d), only the prompts of the non-baseline models are restored by RECORD, and the trajectory distances with the adversarial prompts are averaged over 20 successful restoration attempts.

for denoiser-based erasure methods (ESD), embeddings initialized close to the target prompts tend to diverge from the target prompt embedding, whereas, in the case of text-encoder-based erasure methods (AdvUnlearn), embeddings initialized far from the target prompts tend to converge to it. This suggests that denoiser based erasure methods are mainly effective in suppressing the generation of the erased concept at prompts that are embedded close to the target. For AdvUnlearn initial embeddings (Figure 2a), we use the unlearned text encoder, which leads to radically different (from ESD) initialisations for the target prompt and those perturbed on a token level. However, when appending random characters, or initializing with random characters, AdvUnlearn encodes like the baseline encoder. Despite this, both techniques are as vulnerable to small perturbations (Table 5 in appendix A).

4.4 Semantic Latents

Motivated by the prior literature [26, 37], we also compared the bottleneck and final downsampling features of the U-Net denoiser in the unlearned and baseline models to provide a different perspective to the vulnerability of the unlearned models. We compare trajectories of these features during inference with both the target and restored prompts, and present the cosine similarity between the trajectory of the baseline model from the target prompt and the trajectories of the unlearned / baseline models from the restored / target prompts in Figure 3.

Unlearned models with successfully restored concepts have trajectories as far from the baseline-target trajectory as trajectories generated by unrelated prompts in the baseline model (Figure 3a-b), whereas unlearned models with the non-perturbed target prompt produce trajectories much closer to the baseline model with the same target prompt (Figure 3c-d), despite not rendering van-Gogh-related images. These findings suggest that **there almost always exists some inference trajectories far away from that of the baseline, which an unlearned model can take to generate the unlearned concept**. Consequently, the denoiser-based unlearning methods do not remove information of the concept from the denoiser, but again merely suppress their generation from prompts close to the target prompt.

5 Conclusions

In this study, we introduced RECORD, a novel white-box concept restoration algorithm designed for restoring erased concepts from unlearned text-to-image diffusion models by adversarially perturbing the input prompts. To the best of our knowledge, RECORD is the first algorithm capable of consistently carrying out non-seed-specific concept restoration attacks, outperforming existing restoration methods by up to 17.8 times. Furthermore, our investigation into existing concept erasure techniques revealed that adversarial prompts are pervasive throughout the prompt embedding space. These insights not only underscore a significant vulnerability inherent in current erasure approaches but also pave the way for future research, inspiring the development of new concept erasure and restoration algorithms that can more effectively mitigate or exploit these vulnerabilities.

Acknowledgment

LB, AR, and KZ were supported by the EPSRC Centre for Doctoral Training in Mathematical Modelling, Analysis and Computation (MAC-MIGS) funded by the UK Engineering and Physical Sciences Research Council (grant EP/S023291/1), Heriot-Watt University and the University of Edinburgh. This work was supported by the Edinburgh International Data Facility (EIDF) and the Data-Driven Innovation Programme at the University of Edinburgh. We thank Christos Christodoulopoulos for his useful discussions, and for his input to the Hackathon Workshop on Generative Modeling.

References

- [1] Lucas Beerens and Desmond J Higham. Adversarial ink: Componentwise backward error attacks on deep learning. 89(1):175–196.
- [2] Nicholas Carlini, Milad Nasr, Christopher A. Choquette-Choo, Matthew Jagielski, Irena Gao, Anas Awadalla, Pang Wei Koh, Daphne Ippolito, Katherine Lee, Florian Tramèr, and Ludwig Schmidt. Are aligned neural networks adversarially aligned? In *NeurIPS*.
- [3] Zhi-Yi Chin, Chieh-Ming Jiang, Ching-Chun Huang, Pin-Yu Chen, and Wei-Chen Chiu. Prompting4Debugging: Red-teaming text-to-image diffusion models by finding problematic prompts. In *ICML*, September 2023.
- [4] Kevin Clark and Priyank Jaini. Text-to-image diffusion models are zero-shot classifiers. In *NeurIPS*, March 2023.
- [5] Yinpeng Dong, Fangzhou Liao, Tianyu Pang, Hang Su, Jun Zhu, Xiaolin Hu, and Jianguo Li. Boosting Adversarial Attacks with Momentum.
- [6] Alexey Dosovitskiy, Lucas Beyer, Alexander Kolesnikov, Dirk Weissenborn, Xiaohua Zhai, Thomas Unterthiner, Mostafa Dehghani, Matthias Minderer, Georg Heigold, Sylvain Gelly, Jakob Uszkoreit, and Neil Houlsby. An Image is Worth 16x16 Words: Transformers for Image Recognition at Scale. October 2020.
- [7] Javid Ebrahimi, Anyi Rao, Daniel Lowd, and Dejing Dou. HotFlip: White-box adversarial examples for text classification, May 2018.
- [8] Chongyu Fan, Jiancheng Liu, Yihua Zhang, Eric Wong, Dennis Wei, and Sijia Liu. SalUn: Empowering machine unlearning via gradient-based weight saliency in both image classification and generation. In *ICLR*, October 2023.
- [9] Rinon Gal, Yuval Alaluf, Yuval Atzmon, Or Patashnik, Amit H. Bermano, Gal Chechik, and Daniel Cohen-Or. An image is worth one word: Personalizing text-to-image generation using textual inversion. In *ICLR*, August 2022.
- [10] Rohit Gandikota, Joanna Materzynska, Jaden Fiotto-Kaufman, and David Bau. Erasing concepts from diffusion models. In *ICCV*, March 2023.
- [11] Rohit Gandikota, Hadas Orgad, Yonatan Belinkov, Joanna Materzyńska, and David Bau. Unified concept editing in diffusion models. In *IEEE Workshop/Winter Conference on Applications of Computer Vision*, pages 5099–5108. arXiv, August 2023.

- [12] Chao Gong, Kai Chen, Zhipeng Wei, Jingjing Chen, and Yu-Gang Jiang. Reliable and Efficient Concept Erasure of Text-to-Image Diffusion Models. In *ECCV*, July 2024.
- [13] Chuan Guo, Alexandre Sablayrolles, Hervé Jégou, and Douwe Kiela. Gradient-based Adversarial Attacks against Text Transformers. In *EMNLP*.
- [14] Xiaoxuan Han, Songlin Yang, Wei Wang, Yang Li, and Jing Dong. Probing unlearned diffusion models: A transferable adversarial attack perspective, April 2024.
- [15] Anubhav Jain, Yuya Kobayashi, Takashi Shibuya, Yuhta Takida, Nasir Memon, Julian Togelius, and Yuki Mitsufuji. TraSCE: Trajectory Steering for Concept Erasure, December 2024.
- [16] Eric Jang, Shixiang Gu, and Ben Poole. Categorical reparameterization with gumbel-softmax, August 2017.
- [17] Erik Jones, Anca Dragan, Aditi Raghunathan, and Jacob Steinhardt. Automatically auditing large language models via discrete optimization. In *ICML*, March 2023.
- [18] Changhoon Kim, Kyle Min, and Yezhou Yang. R.A.C.E.: Robust Adversarial Concept Erasure for Secure Text-to-Image Diffusion Model. In *ECCV*, May 2024.
- [19] Changhoon Kim and Yanjun Qi. A Comprehensive Survey on Concept Erasure in Text-to-Image Diffusion Models.
- [20] Nupur Kumari, Bingliang Zhang, Sheng-Yu Wang, Eli Shechtman, Richard Zhang, and Jun-Yan Zhu. Ablating concepts in text-to-image diffusion models. In *ICCV*, March 2023.
- [21] Alexey Kurakin, Ian Goodfellow, and Samy Bengio. Adversarial examples in the physical world. In *ICLR*.
- [22] Alexander C. Li, Mihir Prabhudesai, Shivam Duggal, Ellis Brown, and Deepak Pathak. Your diffusion model is secretly a zero-shot classifier. In *ICCV*, March 2023.
- [23] Hang Li, Chengzhi Shen, Philip Torr, Volker Tresp, and Jindong Gu. Self-Discovering Interpretable Diffusion Latent Directions for Responsible Text-to-Image Generation. In *CVPR*, March 2024.
- [24] Junnan Li, Dongxu Li, Caiming Xiong, and Steven Hoi. BLIP: Bootstrapping language-image pre-training for unified vision-language understanding and generation. In *ICML*, January 2022.
- [25] Mengyao Lyu, Yuhong Yang, Haiwen Hong, Hui Chen, Xuan Jin, Yuan He, Hui Xue, Jungong Han, and Guiguang Ding. One-dimensional adapter to rule them all: Concepts, diffusion models and erasing applications. In *CVPR*, March 2024.
- [26] Yong-Hyun Park, Mingi Kwon, Jaewoong Choi, Junghyo Jo, and Youngjung Uh. Understanding the latent space of diffusion models through the lens of riemannian geometry. In *Proceedings of the 37th International Conference on Neural Information Processing Systems, NIPS '23*, Red Hook, NY, USA, 2023. Curran Associates Inc.
- [27] Minh Pham, Kelly O. Marshall, Niv Cohen, Govind Mittal, and Chinmay Hegde. Circumventing concept erasure methods for text-to-image generative models. In *ICLR*, August 2023.
- [28] Alec Radford, Jong Wook Kim, Chris Hallacy, Aditya Ramesh, Gabriel Goh, Sandhini Agarwal, Girish Sastry, Amanda Askell, Pamela Mishkin, Jack Clark, Gretchen Krueger, and Ilya Sutskever. Learning transferable visual models from natural language supervision. In *ICML*, February 2021.
- [29] Joseph Redmon and Ali Farhadi. YOLOv3: An Incremental Improvement, April 2018.
- [30] Robin Rombach, Andreas Blattmann, Dominik Lorenz, Patrick Esser, and Björn Ommer. High-resolution image synthesis with latent diffusion models, April 2022.
- [31] Olaf Ronneberger, Philipp Fischer, and Thomas Brox. U-Net: Convolutional Networks for Biomedical Image Segmentation. In Nassir Navab, Joachim Hornegger, William M. Wells, and Alejandro F. Frangi, editors, *Medical Image Computing and Computer-Assisted Intervention – MICCAI 2015*, pages 234–241, Cham, 2015. Springer International Publishing.

- [32] Patrick Schramowski, Manuel Brack, Björn Deiseroth, and Kristian Kersting. Safe Latent Diffusion: Mitigating Inappropriate Degeneration in Diffusion Models. In *CVPR*, April 2023.
- [33] Weijia Shi, Xiaochuang Han, Hila Gonen, Ari Holtzman, Yulia Tsvetkov, and Luke Zettlemoyer. Toward Human Readable Prompt Tuning: Kubrick’s *The Shining* is a good movie, and a good prompt too? In *EMNLP*, December 2022.
- [34] Taylor Shin, Yasaman Razeghi, Robert L. Logan Iv, Eric Wallace, and Sameer Singh. Auto-Prompt: Eliciting Knowledge from Language Models with Automatically Generated Prompts. In *EMNLP*, Online, 2020.
- [35] Gowthami Somepalli, Vasu Singla, Micah Goldblum, Jonas Geiping, and Tom Goldstein. Diffusion Art or Digital Forgery? Investigating Data Replication in Diffusion Models. In *CVPR*, December 2022.
- [36] Jiaming Song, Chenlin Meng, and Stefano Ermon. Denoising diffusion implicit models. In *ICLR*, October 2020.
- [37] Viacheslav Surkov, Chris Wendler, Mikhail Terekhov, Justin Deschenaux, Robert West, and Caglar Gulcehre. Unpacking SDXL turbo: Interpreting text-to-image models with sparse autoencoders, October 2024.
- [38] Yu-Lin Tsai, Chia-Yi Hsu, Chulin Xie, Chih-Hsun Lin, Jia-You Chen, Bo Li, Pin-Yu Chen, Chia-Mu Yu, and Chun-Ying Huang. Ring-a-bell! How reliable are concept removal methods for diffusion models? In *ICLR*, October 2023.
- [39] Eric Wallace, Shi Feng, Nikhil Kandpal, Matt Gardner, and Sameer Singh. Universal adversarial triggers for attacking and analyzing NLP, January 2021.
- [40] Jianzhong Wang. *Isomaps*, pages 151–180. Springer Berlin Heidelberg, Berlin, Heidelberg, 2012.
- [41] Yuxin Wen, Neel Jain, John Kirchenbauer, Micah Goldblum, Jonas Geiping, and Tom Goldstein. Hard prompts made easy: Gradient-based discrete optimization for prompt tuning and discovery. In *NeurIPS*, February 2023.
- [42] Jing Wu and Mehrtash Harandi. Scissorhands: Scrub data influence via connection sensitivity in networks. In *ECCV*, January 2024.
- [43] Jing Wu, Trung Le, Munawar Hayat, and Mehrtash Harandi. EraseDiff: Erasing data influence in diffusion models, July 2024.
- [44] Jaehong Yoon, Shoubin Yu, Vaidehi Patil, Huaxiu Yao, and Mohit Bansal. SAFREE: Training-Free and Adaptive Guard for Safe Text-to-Image And Video Generation. In *ICLR*, October 2024.
- [45] Gong Zhang, Kai Wang, Xingqian Xu, Zhangyang Wang, and Humphrey Shi. Forget-me-not: Learning to forget in text-to-image diffusion models. In *CVPR*, Seattle, WA, USA, June 2024.
- [46] Yimeng Zhang, Xin Chen, Jinghan Jia, Yihua Zhang, Chongyu Fan, Jiancheng Liu, Mingyi Hong, Ke Ding, and Sijia Liu. Defensive unlearning with adversarial training for robust concept erasure in diffusion models, May 2024.
- [47] Yimeng Zhang, Jinghan Jia, Xin Chen, Aochuan Chen, Yihua Zhang, Jiancheng Liu, Ke Ding, and Sijia Liu. To generate or not? Safety-driven unlearned diffusion models are still easy to generate unsafe images ... For now. In *ECCV*, October 2023.

A Choice of loss function

We consider two loss functions from literature [3, 27, 47], that are commonly used for identifying adversarial prompts for restoring concepts from unlearned models:

$$L_1(y) = \mathbb{E}_{t,z} \left[\left\| \epsilon_{\theta'}(z_t, t, \mathcal{T}(y)) - \epsilon \right\|_2^2 \right] \quad (3)$$

$$L_2(y) = \mathbb{E}_{t,z} \left[\left\| \epsilon_{\theta'}(z_t, t, \mathcal{T}(y)) - \epsilon_{\theta}(z_t, t, \mathcal{T}(y_{\text{target}})) \right\|_2^2 \right] \quad (4)$$

where z_t is obtained through the forward diffusion process, $z_0 \sim p_{\text{target}}$ is sampled from the target data distribution, y_{target} is the target prompt. L_1 [27] and L_2 [3] are minimized by optimizing prompts y to match the denoiser predictions respectively to: the true noise from the forward diffusion sequence ϵ , or the predicted noise by the baseline denoiser with the target prompt $\epsilon_{\theta}(z_t, t, \mathcal{T}(y_{\text{target}}))$.

To compare both loss functions, we consider the non-seed-specific prompt embedding attack setting:

$$\tilde{L}_1(c) = \mathbb{E}_{t,z} \left\| \epsilon_{\theta'}(z_t, t, c) - \epsilon \right\|_2^2 \quad (5)$$

$$\tilde{L}_2(c) = \mathbb{E}_{t,z} \left\| \epsilon_{\theta'}(z_t, t, c) - \epsilon_{\theta}(z_t, t, c_{\text{target}}) \right\|_2^2. \quad (6)$$

We use NAdam optimizer and iterate over a sampled z_0 set of 100 images 50 times, with a constant learning rate of 0.1 and a batch size of 16. z_0 is generated by the baseline model using the target prompt. Attacks with each loss formulation find 500 adversarial prompt embeddings from random initializations, and generate one image per prompt embedding to be classified in the same setting described in Section 4.1.

The results are presented in Table 5. We notice that, for concepts where the classifier has a high accuracy in classifying the images from the baseline model, as previously shown in Table 2, the \tilde{L}_2 formulation performs marginally better than \tilde{L}_1 . For concepts whose classification accuracy is already low on the baseline model, the difference between the two loss formulations becomes negligible. This suggests when the baseline model can generate more ‘accurate’ images as perceived by the classifier, the outputs of its denoiser can also act as a more informative surrogate to aid the concept restoration process.

When carrying about embedding attacks on AdvUnlearn, which modifies only the text encoder rather than the denoiser, embeddings which can successfully restore concepts are guaranteed to exist. It is thus surprising to observe that in this seemingly easier setting, the ASR on AdvUnlearn is not necessarily higher than other denoiser-based concept erasure methods.

The RECORD algorithm discussed in this paper uses loss (4) by default due to its marginal improvement in the attack performance. Consequently, this particular loss may result in the increased runtime of the RECORD algorithm, as well as requiring access to the baseline model ϵ_{θ} . These limitations, however, can be mitigated or avoided by switching to loss (3) at the expense of a marginally poorer performance.

Erased Concept	Restoration Method	Erasure Method					
		ESD [10]	FMN [45]	AC [20]	SPM [25]	UCE [11]	AdvUnlearn [46]
van Gogh	No attack	3.4	17.6	32.2	45.4	52.8	0.8
	Embed attack 1	99.8	99.8	99.4	100.0	91.4	92.8
	Embed attack 2	99.8	99.8	100.0	99.4	98.4	99.0

Erased Concept	Restoration Method	Erasure Method					
		ESD [10]	ED [43]	SH [42]	SPM [25]	SalUn [8]	AdvUnlearn [46]
Church	No attack	20.2	4.4	1.0	84.6	2.0	1.6
	Embed attack 1	95.6	99.4	22.8	98.0	99.4	96.6
	Embed attack 2	100.0	100.0	64.6	99.8	100.0	100.0
Garbage Truck	No attack	6.2	20.4	9.2	28.4	9.0	0.2
	Embed attack 1	98.0	98.4	18.0	98.0	99.6	96.2
	Embed attack 2	98.8	100.0	3.8	99.6	100.0	92.4
Parachute	No attack	0.8	3.8	2.2	29.8	1.2	0.2
	Embed attack 1	91.2	89.6	4.8	73.6	63.0	46.6
	Embed attack 2	99.4	93.8	1.2	46.6	61.6	44.8

Erased Concept	Restoration Method	Erasure Method					
		ESD [10]	SH [42]	SPM [25]	SalUn [8]	UCE [11]	AdvUnlearn [46]
Nudity	No attack	49.2	2.0	49.6	1.8	41.8	38.4
	Embed attack 1	98.4	83.0	99.6	99.4	96.8	98.6
	Embed attack 2	98.2	87.6	98.6	99.8	98.8	96.8

Table 5: Attack success rate (%) of the embedding attacks for art style, object and nudity attacks. Embed attack 1 and 2 refer to the two loss formulation \tilde{L}_1 and \tilde{L}_2 , respectively.

B Example Images

In this section we present example images generated by different restoration methods, which extends from Table 1, as well as from the embedding attack discussion in Appendix A

Erased Concept	Restoration Method	Erasure Method					
		ESD [10]	FMN [45]	AC [20]	SPM [25]	UCE [11]	AdvUnlearn [46]
van Gogh	No attack						
	Embed attack 1						
	Embed attack 2						

Table 6: Generated images of erased concepts using embedding attacks. Each image column of the same concept is generated using the same latent initialization. Models have unlearned the style of van gogh paintings. Target prompt "a painting in the style of van gogh"

Erased Concept	Restoration Method	Erasure Method					
		ESD [10]	SH [42]	SPM [25]	SalUn [8]	UCE [11]	AdvUnlearn [46]
Nudity	No attack						
	Embed attack 1						
	Embed attack 2						

Table 7: Generated images of erased concepts using embedding attacks. Each image column of the same concept is generated using the same latent initialization. Models have unlearned the concept of nudity. Target prompt asked for nudity.

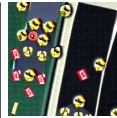
Erased Concept	Restoration Method	Erasure Method					
		ESD [10]	ED [43]	SH [42]	SPM [25]	SalUn [8]	AdvUnlearn [46]
Church	No attack						
	Embed attack 1						
	Embed attack 2						
Garbage Truck	No attack						
	Embed attack 1						
	Embed attack 2						
Parachute	No attack						
	Embed attack 1						
	Embed attack 2						

Table 8: The generated images of erased concepts using embedding attacks. Each image column of the same concept is generated using the same latent initialization. Target prompt "a photorealistic image of *object*"

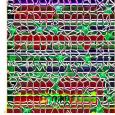
Erased Concept	Restoration Method	Erasure Method					
		ESD [10]	ED [43]	SH [42]	SPM [25]	SalUn [8]	AdvUnlearn [46]
Church	P4D [3]						
	UD [47]						
	RECORD						
Garbage Truck	P4D [3]						
	UD [47]						
	RECORD						
Parachute	P4D [3]						
	UD [47]						
	RECORD						

Table 9: The generated images of erased concepts using prompt attacks. Each image column of the same concept is generated using the same latent initialization. Target prompt "a photorealistic image of *object*"

Table 10: The generated images of erased concepts using prompt attacks. Each image column of the same concept is generated using the same latent initialization. Target prompt asked for nudity.

Erased Concept	Restoration Method	Erasure Method					
		ESD [10]	ED [43]	SH [42]	SPM [25]	SalUn [8]	AdvUnlearn [46]
Nudity	P4D [3]						
	UD [47]						
	RECORD						

C Tokens Length Ablation Study

The number of available tokens for perturbation is an important factor affecting the ASRs of the concept restoration methods. This section showcases the ASR of RECORD with 16 and 32 tokens, as shown in Tables 11 and 12. The rest of the optimization configuration is consistent with that of Section 4.2.

Erased Concept	Prompt Length	Erasure Method					
		ESD [10]	FMN [45]	AC [20]	SPM [25]	UCE [11]	AdvUnlearn [46]
van Gogh	16	26.2	53.8	89.6	85.6	94.2	13.6
	32	40.0	69.6	92.4	91.8	95.4	29.4
	64	64.0	76.8	94.0	95.6	97.6	33.0

Table 11: Attack success rate (%) for models with the van Gogh style erased. Comparing RECORD with different allowed prompt lengths in terms of tokens.

Erased Concept	Prompt Length	Erasure Method					
		ED [43]	ESD [10]	SalUn [8]	SH [42]	SPM [25]	AdvUnlearn [46]
Church	16	34.8	58.0	52.8	4.6	89.4	42.4
	32	43.6	67.0	66.6	5.4	94.8	55.6
	64	61.2	75.2	71.4	8.6	92.2	57.0
Garbage Truck	16	18.8	26.2	43.0	1.6	69.0	63.8
	32	34.0	33.8	60.4	1.0	72.0	59.6
	64	40.8	38.8	58.0	1.0	66.4	50.0
Parachute	16	6.0	31.0	32.8	2.0	45.8	17.2
	32	10.0	36.6	35.4	1.0	55.8	26.2
	64	15.4	44.6	48.8	2.0	60.4	35.6
Nudity	16	3.6	62.2	5.2	23.6	54.8	48.4
	32	2.2	65.0	6.6	22.0	65.8	51.6
	64	2.4	70.6	9.0	21.2	69.0	39.2

Table 12: Attack success rate (%) for models with the concepts Church, Garbage Truck, Parachute, and Nudity erased. Comparing RECORD with different allowed prompt lengths in terms of tokens.